1984ApJ...276..440S

THE ASTROPHYSICAL JOURNAL, 276:440–448, 1984 January 15
© 1984. The American Astronomical Society. All rights reserved. Printed in U.S.A.

THE QUASAR Q2345+007A, B: A CASE FOR THE DOUBLE GRAVITATIONAL LENS?

K. SUBRAMANIAN AND S. M. CHITRE
Tata Institute of Fundamental Research, Bombay
Received 1983 March 3; accepted 1983 June 24

ABSTRACT

The recently reported double quasar Q2345+007A, B, with a large separation $\sim 7''.3$ between its components, is demonstrated to impose stringent constraints on possible gravitational lens models. A single gravitational lens can produce the large separation only if it is placed close to the observer at a redshift $Z \lesssim 0.14$. A model involving two intervening galaxies at different redshifts (the double lens) is studied and shown to account for the observed features with reasonable values for the lens parameters. The effects of a cluster are also considered in some detail. Observational tests for distinguishing between various scenarios are suggested; in particular, the time delay between the two images turns out to have opposite signs for the single lens and double lens models.

Subject headings: gravitation — quasars

I. INTRODUCTION

The properties of gravitational lenses are a direct consequence of the gravitational deflection of light which was predicted by the theory of general relativity over 50 years ago. But it was only after the discovery of the double quasar Q0957+561A,B (Walsh, Carswell, and Weymann 1979) and the triple quasar Q1115+080A,B,C (Weymann *et al.* 1980) that their significance came to be appreciated. The observations of gravitational lenses promise to be valuable probes for studying the nature of galaxies and clusters of galaxies, especially for estimating their masses and density distribution.

In an earlier paper (Narasimha, Subramanian, and Chitre 1982, hereinafter referred to as Paper I), we investigated a model for the triple quasar based on a single spheroidal gravitational lens. For this purpose we adopted the complex formalism of Bourassa, Kantowski, and Norton (1973) and Bourassa and Kantowski (1975) and a realistic density distribution for the lens galaxy, to demonstrate that an image configuration in reasonable accord with the observed features of the triple quasar can be produced. In this paper we use techniques developed in Paper I, to examine models for a third gravitational lens, namely the quasar Q2345+007A,B recently reported by Weedman *et al.* (1982). This system is made up of two images with approximate magnitudes of 19.5 and 21, which are separated by $7''.3$; they have nearly identical redshifts of 2.152 and 2.147, with an uncertainty of ± 0.005. The separation of $7''.3$ between the two components of the quasar Q2345+007A,B is the largest image separation observed so far in multiple quasar systems. It turns out that it is this large image separation that sets stringent constraints on theoretical lens models. We illustrate this first with a point lens model. The separation between the images caused by a point lens of mass M is given by (Refsdal 1964),

$$\alpha_0 = 4\left(\frac{GMD_{ds}}{c^2 D_d D_s}\right)^{1/2}, \qquad (1)$$

where D_d and D_s denote respectively distances from the observer to the deflector and source in a Robertson–Walker universe and D_{ds} the deflector-source distance. If we express M in units of $10^{11}\,M_\odot$ (of the order of galactic mass) and the D's in Mpc, we can express α_0 as

$$\alpha_0 = 1''.8\left(\frac{M}{10^{11}\,M_\odot}\right)^{1/2}\left(\frac{1000\ \mathrm{Mpc}}{D_s}\right)^{1/2}\left(\frac{D_{ds}}{D_d}\right)^{1/2}. \qquad (2)$$

For the newly discovered double quasar at the redshift $Z_s = 2.15$, the distance $D_s \approx 2250$ Mpc (assuming $H_0 = 60$ km s^{-1} Mpc^{-1}, $q_0 = 0$) and adopting $D_{ds} \sim D_d$ and $\alpha_0 = 7''.3$, we get for the lens mass,

$$M \approx 37 \times 10^{11}\,M_\odot. \qquad (3)$$

This mass is somewhat large compared to the usual galactic masses. Further, such a massive lens galaxy should be detectable unless M/L for the galaxy is abnormally large (>1000). Indeed, the mass can be decreased by bringing the lens closer, i.e., by decreasing D_d/D_{ds} in equation (1). However, since the intensity, I, of light from the galaxy scales as $\sim L/D_d^2$, where L is the intrinsic luminosity of the galaxy, and $L \propto M$, we have $I \propto 1/(D_{ds} D_d)$, which is minimized when $D_d \sim D_{ds}$ (corresponding to a redshift of ~ 0.45 in the present case). Thus, bringing the lens closer would make its detection easier. However, as yet no lens galaxy has been found; and if this situation continues to hold, it will not auger well for the lens models.

In this paper we consider a double gravitational lens model involving two intervening galaxies at different redshifts. A crucial question concerning the double lens models is their low probability which should be compared with probability of simply finding two QSOs within $7''.3$ of each other. For this purpose we follow the method of Gott and Gunn (1974) and estimate the probability of having a quasar within a cricle of radius $7''.3$ centered at a random point in the sky to be $\sim 2.6 \times 10^{-4}$ considering the fact that one of the QSOs has a magnitude of 21. We shall see later that this probability turns out to be smaller than that of having two extended deflectors in the form of galaxies en route to a distant quasar.

The rest of the paper is arranged as follows. In § II we consider a model involving a single galaxy and show that unless we place the lens very close to the observer, no solutions with

© American Astronomical Society • Provided by the NASA Astrophysics Data System

1984ApJ...276..440S

reasonable values for the parameters of the galaxy are possible. We then proceed to consider a model involving two intervening galaxies at different redshifts. The mathematical formalism for this case, which we shall refer to as the double lens, is given in § III in some detail along with the numerical results. Here we also consider a special case of the double lens model, where the two galaxies are at roughly the same redshift—a situation that could arise, for example, if the galaxies are members of a small group of galaxies (or a cluster). The effects of a cluster are studied in § IV in the framework of a lens model involving a single galaxy in a cluster. Finally, the last section contains discussion of the results along with our conclusions.

II. THE SINGLE LENS MODEL

First we shall attempt to model the observed properties of Q2345+007A,B with a single galaxy acting as a lens. The mathematical formalism is as in Bourassa, Kantowski, and Norton (1973), Bourassa and Kantowski (1975), and Paper I, where we define a complex function, $I(x_0, y_0)$ called the scattering function, which incorporates all the information we need about the lens properties. The source and image positions, projected onto the deflector plane which is taken perpendicular to the line of sight, are described by the complex numbers $z = x + iy$ and $z_0 = x_0 + iy_0$, respectively (see Fig. 1 in Paper I). These are related by the equation

$$z = z_0 - \frac{4GD}{c^2} I^*(x_0, y_0) , \tag{4}$$

where $D = D_d D_{ds}/Ds$. For a given source position z, roots of equation (4) give the number and location of images, z_0's.

For the purpose of computation we adopt as in Paper I a galactic model with eccentricity e and a density distribution which is taken to be the truncated King model (King 1972):

$$\begin{aligned} \rho(r) &= \rho_0(1 + r^2/r_c^2)^{-3/2} , \quad r/r_c \le n \\ &= 0 \qquad\qquad\qquad\quad , \quad r/r_c > n . \end{aligned} \tag{5}$$

Inserting the density distribution into the expression for the scattering function, we get

$$I(x_0, y_0) = \frac{M}{r_c} f(x_0, y_0) , \tag{6}$$

where the function $f(x_0, y_0)$ is derived in Paper I. Here all the quantities A_0, B_0, x_0, and y_0 have been expressed in units of the core radius r_c.

We also define the line-of-sight velocity dispersion following Young *et al.* (1981) to be

$$\sigma_v^2 = 4\pi G \rho_0 a^2 , \tag{7}$$

where a is the structural length and is equal to $r_c/3$, and ρ_0 is the central density. Defining $\delta = \ln[(n^2 + 1)^{1/2} + n] - n/(n^2 + 1)^{1/2}$, we get

$$\sigma_v = \left[\frac{GM}{9r_c(1 - e^2)^{1/2}\delta}\right]^{1/2} . \tag{8}$$

Using the scattering function given by equation (6) and expressing the source position $z = x + iy$, in units of r_c, equation (4) takes the form

$$z_0^* = z^* + \mu f(x_0, y_0) \quad \left(\mu = \frac{4GMD}{r_c^2 c^2}\right) , \tag{9}$$

the roots of which for a specified value of z give the location of images. The parameters to be fixed before one solves this equation are μ, $e \sin \gamma$, and n. From our extensive numerical computation with the single lens model, we find that if multiple images are formed, the magnitude of the image separation in units of r_c is not very sensitive to the eccentricity of the lens and the changes in the source position. It depends only on the value of the parameter μ in equation (9). The change in either $e \sin \gamma$ or z, however, alters the geometry of the image configuration. For example, if $e \sin \gamma = 0$, then the images lie in a straight line, while for a typical solution for the triple quasar discussed in Paper I the images lie roughly at the vertices of a triangle with $e \sin \gamma = 0.6$. This simplifies greatly the search for those solutions of equation (9) which give the observed image separation.

We assume a spherical lens at a redshift, say Z_d, and for each specified value of μ we find the value of z_0 for which z becomes 0. We need to search only along one line passing through the origin, say the x-axis, since for a spherically symmetric lens the solution to equation (5), with $z = 0$, is a circle in the image plane $|z_0| = \text{constant} = b$ (say). The angular image separation is then $2br_c/D_d$; and by demanding that this be equal to 7".3 one can find r_c. Since the redshift of the lens has already been fixed, one can calculate $D = D_d D_{ds}/D_s$ for a chosen cosmological model. This enables us to calculate M from $M = \mu r_c^2 c^2/4GD$ and σ_v from equation (8). The results for various values of μ and Z_d are summarized in Table 1, for the following choice of the parameters; $n = 20$, $H_0 = 60$ km s^{-1} Mpc^{-1}, $q_0 = 0$. In Table 1 the mass M has been expressed in units of $10^{11}\ M_\odot$, σ_v in units of km s^{-1}, and r_c in units of kpc. The dark lines enclose regions where $M \lesssim 20 \times 10^{11}\ M_\odot$ and $\sigma_v \lesssim 400$ km s^{-1}, which we adopt as "reasonable" limits for parameters appropriate for a galaxy.

We see from Table 1 that unless the lens is placed quite close to the observer with redshifts $Z_d \lesssim 0.14$, it is not possible to get the observed 7".3 separation with reasonable values for the mass and velocity dispersion of the galaxy. One should also remember that at the redshift of 0.1, a galaxy of mass $\sim 15 \times 10^{11}\ M_\odot$ should be easily observable, unless M/L for the galaxy is large ($\gtrsim 900$).

Nevertheless, we discuss a solution using a single galaxy as the lens which explains both the separation ($\sim$7".3) and the observed intensity ratio between the two images (i.e., $I_a/I_b = 4$–6). The numerical method for arriving at the solution is as adopted in Paper I, and it will be sketched briefly later in § III*b* when we deal with the double lens. The formulae for computing amplifications are adopted from Paper I. Since there are only two images, there is no need to invoke the eccentricity of the galaxy as was the case with the triple quasar. We have therefore taken the lens galaxy to be spherically symmetric, in which case the source and the images lie on a straight line passing through the origin, which has been taken to be the x-axis.

A distributed lens produces an odd number of images and therefore one has to either make one of the images in the three image region faint or two images to be so close to each other to be indistinguishable. The former alternative is not possible if an intensity ratio of 4–6 between the extreme images is to be obtained. Therefore our bright image a is actually made up of two images a_1 and a_2 separated by $\sim$0".1. (This situation is

© American Astronomical Society • Provided by the NASA Astrophysics Data System

1984ApJ...276..440S

TABLE 1

PARAMETERS[a] OF THE SINGLE LENS FOR DIFFERENT μ AND Z_d

	Z_d						
μ	0.05	0.1	0.14	0.18	0.23	0.3	0.5
10:							
M	19.4	38.4	53.4	68.2	86.8	112.9	190.1
σ_v	335	357	366	375	385	400	445
r_c	2.84	5.31	7.05	8.62	10.4	12.49	17.00
20:							
M	9.9	19.5	27.2	34.7	44.2	57.5	96.8
σ_v	349	359	368	376	387	402	447
r_c	1.44	2.68	3.56	4.35	5.23	6.30	8.58
35:							
M	7.3	14.4	20.0	25.6	32.6	42.4	71.4
σ_v	372	383	392	401	413	429	476
r_c	0.93	1.74	2.31	2.825	3.40	4.09	5.57
50:							
M	6.3	12.5	17.4	22.2	28.3	36.7	61.8
σ_v	392	404	414	423	435	451	502
r_c	0.73	1.35	1.80	2.20	2.65	3.19	4.33
65:							
M	5.8	11.4	15.9	20.3	25.8	33.5	56.5
σ_v	410	422	432	441	454	471	525
r_c	0.61	1.14	1.51	1.84	2.22	2.67	3.63
80:							
M	5.4	10.7	14.9	19.0	24.2	31.5	53.0
σ_v	425	437	448	457	471	489	544
r_c	0.53	0.99	1.32	1.61	1.94	2.33	3.17
100:							
M	5.1	10.1	14.0	17.9	22.8	29.6	49.9
σ_v	442	455	466	477	490	509	566
r_c	0.46	0.86	1.14	1.40	1.68	2.02	2.75
130:							
M	4.8	9.4	13.1	16.8	21.4	27.8	46.8
σ_v	465	478	489	501	515	535	595
r_c	0.39	0.73	0.97	1.19	1.43	1.72	2.34
160:							
M	4.6	9.0	12.6	16.1	20.5	26.6	44.8
σ_v	484	499	510	522	537	558	621
r_c	0.35	0.64	0.86	1.05	1.26	1.52	2.06

[a] The dark lines enclose the region of acceptable lens parameters.

analogous to the single lens model of the double quasar 0957+561A,B.) As we shall see later, the above feature of the single lens model provides us with a handle in the form of the time delay for observationally distinguishing it from all the other models considered subsequently. The position of the bright image a has been fixed by taking the average of the positions of a_1 and a_2 weighted with respect to their intensities, and the intensity of a by merely adding the intensities of a_1 and a_2. We have also worked out the time delay between the images using the expressions given by Cooke and Kantowski (1975). A sample solution for a single lens is given in Table 2. We note that the values of mass and velocity dispersion shown here for an explicit sample solution with $\mu = 35$, $Z_d = 0.1$ are in accord with those in Table 1. This also substantiates our claim that the image separation is only weakly dependent on the source position, an assumption used to calculate the parameters in Table 1. If subsequent observations reveal a lens galaxy at a redshift $Z \gtrsim 0.2$, then Table 1 predicts that this galaxy alone is not capable of explaining the observations (i.e., separation of 7″.3), and an extra component to the lens is required. We are inclined to believe that a single lens galaxy is unlikely to image the observed configuration under normal circumstances, though it cannot be ruled out. In the next section we consider this extra component in the form of another galaxy intercepting the light rays during their paths to the observer. This enables us to push the lenses further from the observer and also reduces the mass and velocity dispersion of the lens galaxy.

III. THE DOUBLE LENS

We now consider the case where the lens is made up of two galaxies capable of gravitationally deflecting the light rays from the source and focusing them on to the observer. We saw in the previous section that to explain the 7″.3 separation with a single galaxy at $Z_d \lesssim 0.14$, one requires the galaxy to have unreasonably large values of the mass and velocity dispersion. However, if we have an additional intervening galaxy, it will further bend light rays from the source, and this can lead to an increase in the image separation. Since each galaxy in this picture need produce only part of 7″.3 image separation, the requirement on the mass and velocity dispersion of the lens galaxy is correspondingly reduced. This also means that the lenses can be pushed further away from the observer and can still explain the observed separation with reasonable values of

© American Astronomical Society • Provided by the NASA Astrophysics Data System

1984ApJ...276..440S

TABLE 2

SAMPLE SOLUTION FOR SINGLE LENS

Parameter	Value
Z_d	0.1
μ	35
n	20
Image position:	
a_1	−1.349
a_2	−1.267
$a = (a_1 + a_2)/2$	−1.310
b	7.17
Amplification:	
a_1	−3.709
a_2	3.334
a	7.043
b	1.563
Intensity ratio	4.51
θ_{ab}	7.″3
$\theta_{a_1a_2}$	0.″07
Mass	$15.61 \times 10^{11}\ M_\odot$
Velocity dispersion (σ_v)	391 km s^{-1}
Core radius r_c	1.81 kpc
Time delay:	
$t_b - t_a$	−0.98 yr
$t_{a_1} - t_{a_2}$	3.47×10^{-6} yr

NOTE.—The position of the bright image a is fixed by taking the average of a_1 and a_2, weighted with respect to their intensities; the intensity of a is fixed by adding the intensities of a_1 and a_2.

the lens parameters. We shall now set up a detailed formalism in order to examine the viability of this double-lens scenario.

a) *Mathematical Formulation*

We use the basic ideas of Bourassa *et al.* (Bourassa, Kantowski, and Norton 1973; Bourassa and Kantowski 1975) and extend their formalism to the case of the double lens. The scheme for bending photon paths from the source by two intervening lens galaxies is illustrated in Figure 1. Here we trace the path of a light ray which starts at the source S, gets deflected by lens A at Q and by lens B at P before reaching the observer at O. The line PQ when extended backward cuts the source plane at R, and the line OP cuts the source plane at I, which is the position of the image. Note that the lens A, the lens B, and the observer need not be aligned. This is taken into account by positioning B at point u in Figure 1 which is displaced from the origin of the plane of the second deflector. Assuming that the distances between the deflectors, the source and the observer are larger than the impact parameter distances the bending angles α_A and α_B defined by Bourassa *et al.* have negligible component parallel to the photon path i.e., the z-axis in Figure 1. The position vectors of S, R, and I can be now related for small bending angles by the following equations:

$$r_S = r_R + D_{AS}\,\alpha_A(r_Q)$$
$$r_R = r_I + D_{BS}\,\alpha_B(r_P - r_u)\,. \qquad (10)$$

The two-component nature of all the vectors in equation (10) allows one to adopt a complex representation for the quantities involved. Let the vectors r_S, r_R, r_I, r_P, r_Q, and r_u be represented by the complex numbers $\tilde{z}$, v, w, z_0, v_0 and u, respectively. Then equations (10) can be cast in the form

$$\tilde{z} = v - \frac{4GD_{AS}}{c^2}\,I_A^*(v_0)\,,$$
$$v = w - \frac{4GD_{BS}}{c^2}\,I_B^*(z_0 - u)\,, \qquad (11)$$

where I_A and I_B are the single lens scattering functions of A and B described in § III. At this stage we relate r_Q to r_P and r_R by extending PQR to the point O′ and noting that $r_Q = D_{AO'}/D_{SO'}\,r_R = D_{AO'}/D_{BO'}\,r_P$. With a given cosmological model, we can eliminate all reference to the point O'. We restrict ourselves to $q_0 = 0$ and zero pressure model to get, after a lengthy but straightforward computation, the following relation:

$$r_Q = \frac{D_{AS}}{D_{BS}}\,r_P + \frac{D_{AB}\,(1 + Z_A)}{D_{BS}\,(1 + Z_S)}\,r_R \qquad (12)$$

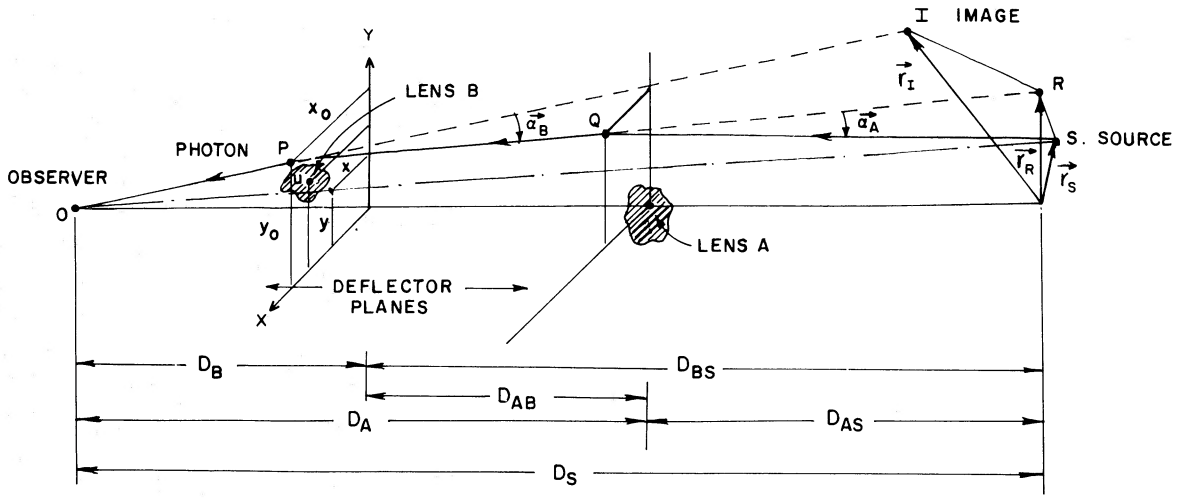

FIG. 1.—Schematic representation of the double lens consisting of two lens galaxies A and B, along with the position of the observer, source, and image. The photon path is essentially along the z-axis with the origin chosen to coincide with the projected center of lens A. Lens B, which is located at point U, has been misaligned with respect to the origin.

© American Astronomical Society • Provided by the NASA Astrophysics Data System

1984ApJ...276..440S

or

$$v_0 = \frac{D_{AS}}{D_{BS}} z_0 + \frac{D_{AB}}{D_{BS}} \frac{(1+Z_A)}{(1+Z_S)} v \,. \tag{13}$$

Further we note that r_P is the projection of r_I onto the plane of the second deflector and hence

$$r_P = \frac{D_B}{D_S} r_I \,, \quad \text{or} \quad z_0 = \frac{D_B}{D_S} w \,. \tag{14}$$

We also project the source position onto the plane of the second deflector and define

$$z = \frac{D_B}{D_S} \tilde{z} \,. \tag{15}$$

The set of equations (10)–(15) can be used to transfer all the quantities onto the plane of the second deflector and to write the relation between source position z and image position z_0 as

$$z = z_0 - \mu_B f_B^*(z_0 - u) - \mu_A f_A^*(v_0) \,, \tag{16}$$

where

$$v_0 = Az_0 - \mu_c f_B^*(z_0 - u) \,,$$

$$A = \frac{D_{AS}}{D_{BS}} + \frac{D_S D_{AB}(1+Z_A)}{D_B D_{BS}(1+Z_S)} \,,$$

$$\mu_A = \frac{4GM_A D_{AS} D_B}{r_c^2 c^2 D_S} \,,$$

$$\mu_B = \frac{4GM_B D_{BS} D_B}{r_c^2 c^2 D_S} \,,$$

and

$$\mu_c = \frac{4GM_B D_{AB}(1+Z_A)}{r_c^2 c^2 (1+Z_S)} \,. \tag{17}$$

Here we have assumed the same core radius for both the galaxies and have expressed z, z_0, and u in units of r_c.

The roots of equation (16) for fixed values of z and u give the position of the images formed by the double lens.

The amplification of the images can be found by varying the source position in equation (16) over a small region and finding the corresponding variation in the image position. In the matrix notation we have

$$\begin{pmatrix} \delta x \\ \delta y \end{pmatrix} = T \begin{pmatrix} \delta x_0 \\ \delta y_0 \end{pmatrix} \,,$$

where

$$T = \begin{pmatrix} \mathrm{Re}\,\dfrac{\partial z}{\partial x_0} & \mathrm{Re}\,\dfrac{\partial z}{\partial y_0} \\ \mathrm{Im}\,\dfrac{\partial z}{\partial x_0} & \mathrm{Im}\,\dfrac{\partial z}{\partial y_0} \end{pmatrix} . \tag{18}$$

The amplification, which is the ratio of the projected area of the image to that of the source, is given by

$$\mathrm{Amp} = \frac{1}{\mathrm{Det}\,(T)} \,. \tag{19}$$

The time delay between various images, for the double lens can be worked out in the same manner as that for the single lens. The time delay is the combination of a delay caused by the difference in geometrical path length and a delay resulting from the different gravitational potential wells through which the photon travels. The path length difference is straightforward to calculate, and to the relevant order, each ray consists of three straight lines, namely, OP, PQ, and QS of Figure 1. For images seen at positions $z_{0\alpha}$ and $z_{0\beta}$, the time delay due to differences in geometrical path lengths is

$$c(t_\alpha - t_\beta)_g = f_\alpha - f_\beta \,,$$

where

$$f_i = r_c^2 \left\{ \frac{1}{2} \frac{|v_{0i} - z(D_A/D_B)|^2}{D_S - D_A} + \frac{1}{2} \frac{|z_{0i} - z|^2}{D_B} + \frac{1}{2} \frac{[\,|z_{0i} - z| - |v_{0i} - z(D_A/D_B)|\,]^2}{D_A - D_B} \right\} . \tag{20}$$

In the absence of the third term, and when $D_A = D_B$, it can be easily seen that the above expression reduces to the one for a single lens. The potential part of the time delay is the sum of delays caused by the gravitational influence of galaxy A and galaxy B. The potential time delay depends linearly on the gravitational potential, and hence with the single galaxy time delay given by Cooke and Kantowski (1975) we can write the potential time delay for the double lens as

$$c(t_\alpha - t_\beta)_P = g_\beta - g_\alpha \,,$$

where

$$g_i = \frac{4GM_A}{c^2}(1+Z_A) \int_0^{|v_{0i}|} \frac{f(B)dB}{B} + \frac{4GM_B}{c^2}(1+Z_B) \int_0^{|z_{0i}-u|} \frac{f(B)dB}{B}$$

and

$$f(B) = 1 - \frac{1}{2\delta} \ln \left[\frac{(n^2+1)^{1/2} + (n^2 - B^2)^{1/2}}{(n^2+1)^{1/2} - (n^2 - B^2)^{1/2}} \right] + \frac{1}{\delta} \frac{(n^2 - B^2)^{1/2}}{(n^2+1)^{1/2}} \,. \tag{21}$$

While deriving the expressions for the time delays, the two galaxies have been assumed to be spherical, as this is the case for which we shall present explicit solutions in what follows. The arrival time of light rays from image α minus the arrival time from image β is then given by combining equations (20) and (21), namely,

$$(t_\alpha - t_\beta) = (t_\alpha - t_\beta)_g + (t_\alpha - t_\beta)_P \tag{22}$$

b) *Numerical Results*

We first locate the roots of equation (16) which give images consistent with the observed image separation and intensity ratios. As in § II, we first vary the values of μ and Z_d to find those regions of the parameter space which can account for the observed 7".3 image separation with reasonable values for the lens mass and velocity dispersion. The procedure for this search is analogous to the one adopted in § II for the case of the single lens and is outlined below.

© American Astronomical Society • Provided by the NASA Astrophysics Data System

1984ApJ...276..440S

The two spherical galaxies forming the double lens are taken to be aligned with the observer and the source. An estimate of the image separation produced by a particular combination of the double lens parameters is obtained by finding out the radius of the largest circle $|z_0| = b$ (say), produced in the image plane, when $z = 0$ and $u = 0$. The image separation is then given by $2br_c/D_d$. This is adjusted to 7".3 by varying r_c, and this value of r_c is used to find the masses and velocity dispersion of the lens from (16) and (8). The exact solutions that we get indicate that when the lenses are misaligned, the image configurations are more complicated, but the above method still gives a rough idea of the image separation. After finding out the values of μ and Z_d for which the 7".3 separation can be accounted for, we go on to obtain exact converged solutions. A sample of these solutions is set out in Table 3. The numerical method used to obtain these solutions is sketched below. We consider the lines $x =$ constant and $y =$ constant corresponding to various source positions. These lines go over to a set of curves in the image plane x_0–y_0 plane). The points of intersection of the curve $x = \gamma$ (say) and $y = \delta$ in the image plane give the location of the images for a source position (γ, δ). This helps in the search for the approximate location of the images. We also find numerically the source position and intensity for values of z_0 spanning the image plane. With the help of this we select those regions of the image plane where the observed separation and intensity ratios are satisfied to a reasonable accuracy. In order to get the exact image positions, we use the Muller iteration method (Wilkinson 1965) which is continued until an accuracy of one part in 1000 is achieved. Each root is computed separately, and therefore there is no deflation of the roots. Using the exact image positions, we compute the intensities and time delays with the help of the formulae given in § IV. We also work out the exact image separation in units of r_c and find the value of r_c by demanding that the image separation be equal to 7".3. The mass and the velocity dispersions of the galaxies can then be calculated using equations (16) and (8).

It should be noted that even though the two galaxies have been taken to be spherical, they are not both aligned with the observer, and this introduces departures from the spherical symmetry of the lens. The image configurations, for arbitrary source positions, are therefore complicated. However, in order to simplify the search for solutions, we have taken the source position to lie on the line joining the two projected lens centers, and the misalignment to be such that all the images also lie along the same straight line. The misalignment of the

TABLE 3

TYPICAL SOLUTIONS FOR THE DOUBLE LENS MODEL

No.	Specifications of the Double Lens	Source Position in Units of Core Radius		Image Positions in Units of Core Radius			Amplification	Intensity Ratio
		x	y		x_0	y_0		
I	$Z_A = 0.45$, $Z_B = 0.18$	1.1	1.1	a	7.92	7.92	31.999	$a/b = 5.324$
	$\mu_A = 49$, $\mu_B = 65$			c_1	1.42	1.42	0.021	$c_1/b = 0.003$
	$u = (1.75, 1.75)$, $n = 20$			c_2	−0.66	−0.66	−0.282	$c_2/b = 0.045$
				c_3	−2.13	−2.13	0.018	$c_3/b = 0.003$
				b	−5.86	−5.86	−6.011	
	$r_c = 1.28$ kpc, $M_A = 9.88 \times 10^{11}\ M_\odot$, $M_B = 9.78 \times 10^{11}\ M_\odot$, $\sigma_A = 370$ km s^{-1}, $\sigma_B = 368$ km s^{-1}, $t_b - t_a = 0.281$ yr							
II	$Z_A = 0.45$, $Z_B = 0.18$	0.65	0.65	a	4.13	4.13	36.562	$a/b = 5.89$
	$\mu_A = 16.5$, $\mu_B = 24.5$			c_1	0.48	0.48	0.42	$c_1/b = 0.068$
	$u = (1.0, 1.0)$, $n = 20$			c_2	−0.18	−0.18	−1.202	$c_2/b = 0.194$
				c_3	−0.79	−0.79	0.368	$c_3/b = 0.054$
				b	−2.89	−2.89	−6.207	
	$r_c = 2.51$ kpc, $M_A = 12.80 \times 10^{11}\ M_\odot$, $M_B = 14.2 \times 10^{11}\ M_\odot$, $\sigma_A = 301$ km s^{-1}, $\sigma_B = 316$ km s^{-1}, $t_b - t_a = 0.312$ yr							
III	$Z_A = 0.45$, $Z_B = 0.18$	5.0	5.0	a	9.48	9.48	1.471	$a/b = 5.428$
	$\mu_A = 49$, $\mu_B = 43.5$			c_1	−1.94	−1.94	0.023	$c_1/b = 0.085$
	$u = (1.5, 1.5)$, $n = 20$			b	−3.11	−3.11	−0.271	
	$r_c = 1.40$ kpc, $M_A = 11.81 \times 10^{11}\ M_\odot$, $M_B = 7.82 \times 10^{11}\ M_\odot$, $\sigma_A = 387$ km s^{-1}, $\sigma_B = 315$ km s^{-1}, $t_b - t_a = 2.822$ yr							
IV	$Z_A = 0.45$, $Z_B = 0.3$	4.4	4.4	a	8.74	8.74	1.611	$a/b = 4.183$
	$\mu_A = 40$, $\mu_B = 40$			c_1	−1.05	−1.05	0.029	$c_1/b = 0.075$
	$u = (1.5, 1.5)$, $n = 20$			b	−2.11	−2.11	−0.385	
	$r_c = 2.23$ kpc, $M_A = 16.91 \times 10^{11}\ M_\odot$, $M_B = 14.40 \times 10^{11}\ M_\odot$, $\sigma_A = 367$ km s^{-1}, $\sigma_B = 338$ km s^{-1}, $t_b - t_a = 3.28$ yr							
V	$Z_A = 0.5$, $Z_B = 0.3$	4.9	4.9	a	9.31	9.31	1.523	$a/b = 4.716$
	$\mu_A = 40$, $\mu_B = 45$			c_1	−1.45	−1.45	0.037	$c_1/b = 0.115$
	$u = (1.5, 1.5)$, $n = 20$			b	−2.71	−2.71	−0.323	
	$r_c = 2.13$ kpc, $M_A = 16.17 \times 10^{11}\ M_\odot$, $M_B = 14.70 \times 10^{11}\ M_\odot$, $\sigma_A = 367$ km s^{-1}, $\sigma_B = 350$ km s^{-1}, $t_b - t_a = 3.81$ yr							

© American Astronomical Society • Provided by the NASA Astrophysics Data System

1984ApJ...276..440S

lenses characterized by u, is taken to be of the order of the core radius r_c of each lens galaxy. We find that two types of solutions, satisfying all the required criteria, are possible. The first of these, which we call type I solution, occurs when the projected source position z is between the projected galactic centers, i.e., between o and u. And the second kind, denoted by type II, is yielded when z is far out from both the lenses. For type I solutions we find that there are normally five images, while for type II there are three. In both cases the secondary images are much fainter than the two extreme bright images. From the tables we find that these two kinds of solutions can also be differentiated by the time delay that they predict. Type I solutions predict a time delay of the order of 4 months, whereas the corresponding time delay, for type II is of the order of 3–4 years. Further, we find that in the case of type I a small change in source position results in large variations in amplifications, but this is not the case for type II. This clearly demonstrates that the range of source positions for which a satisfactory solution is obtained is much larger for type II than for type I. On probability grounds also type II is favored owing to the fact that the source can be quite far out (~ 10 kpc) from the projected centers of the galaxies.

Finally we note from the results of Table 3 that not only are the masses and velocity dispersions of the lens galaxies reduced for the double lens from that of a single lens, but also the lenses can be much further out. We have in fact given a sample solution where the lens nearest to us is at a redshift of 0.3. For this solution the distance to the nearest lens has increased by a factor of ~ 2 from that corresponding to the single lens solution presented in § II. This will mean that the nearest galaxy of the double lens will be ~ 1.5 mag fainter (assuming a uniform M/L value).

c) *The Double Lens: Galaxies at the Same Redshift*

We now consider the case when both the lens galaxies forming the double lens are almost at the same redshift. This could arise if a small group of galaxies lies in between the quasar and the observer. We set the distance between the two galaxies to be 2 Mpc for the same of illustration. The results turn out to be quite insensitive to this choice and depend only on μ_A and μ_B. On scanning the parameter space we find that reasonable solutions obtain up to a lens redshift of ~ 0.45. We present below a sample solution with two identical galaxies A, B with the following parameter values:

$$Z_A = 0.4\,, \quad Z_B = 0.4\,, \quad D_{AB} = 2\ \text{Mpc}\,, \quad n = 20\,,$$

$$\mu_A = 40\,, \quad \mu_B = 40\,, \quad u = (1.5, 1.5)\,.$$

The image configuration for a source position (5.5, 5.5) is given in Table 4. We therefore conclude that such a double lens is a plausible scenario which has the merit that the redshift of the lens galaxies can go up to ~ 0.4, much larger than the redshift of the single lens model.

TABLE 4

IMAGE CONFIGURATION FOR A SOURCE POSITION (5.5, 5.5)

Parameter	Value
Image position:	
a	(9.590, 9.590)
c	(−0.225, −0.225)
b	(−1.984, −1.984)
Amplification:	
a	1.428
c	0.023
b	−0.272
I_a/I_b	5.242
I_c/I_b	0.085
M_A	$18.8 \times 10^{11}\ M_\odot$
M_B	$18.8 \times 10^{11}\ M_\odot$
σ_A	355 km s^{-1}
σ_B	355 km s^{-1}
r_c	2.65 kpc
$t_b - t_a$	4.36 yr

IV. THE EFFECTS OF A CLUSTER

In the case of the first lensed quasar (namely, the double quasar Q957+561A,B) a search for the deflector revealed the existence of a cluster of galaxies along the line of sight which was also important in accounting for the observed properties of the images. We have therefore examined whether the presence of a cluster component in the lens models for the present case eases the constraints on the parameters of the lenses. When the lens consists of a galaxy and a cluster at the same redshift, equation (16) becomes

$$z = z_0 - \frac{4GM_g D}{r_c^2 c^2} f^*(z_0) - \frac{4GM_c D}{r_c R_c c^2} f^*\left(\frac{z_0 - u}{R}\right), \quad (23)$$

where M_g is the galaxy mass, M_c the cluster mass, r_c the galactic core radius, R_c the cluster core radius, R is the ratio R_c/r_c, and D is as defined in Equation (4). We have also taken the cluster to have the same density distribution as the galaxy, in which case its velocity dispersion will be given by equation (8) with M_c and R_c in place of M and r_c. We define μ_g and μ_{cl} by

$$\mu_g = \frac{4GM_g D}{r_c^2 c^2}\,, \quad \mu_{cl} = \frac{4GM_c D}{r_c R_c c^2}\,. \quad (24)$$

A particular lens configuration is specified by giving the values of three parameters, namely, μ_g, μ_{cl}, and R. Once again the parameter space is scanned in search of solutions with reasonable lens parameters. For the cluster we demand that the velocity dispersion be $\lesssim 1000$ km s^{-1}, the mass to be $\lesssim 10^{15}\ M_\odot$, and $R_c \sim 200$–400 kpc (with the radius of the cluster equal to $10R_c$). We find that for each fixed R and $\mu_g = 0$, there is a critical value for μ_{cl} beyond which the cluster can itself produce multiple images, with large image separations (for $R = 200$, μ_{cl}[critical] ≈ 800). If we were to adjust the image separation in this case to 7″.3, implausible values of the cluster parameters would be required. Further, for these values of μ_{cl} the velocity dispersion of the cluster is high ($\gtrsim 1100$ km s^{-1}, with $R_c \sim 250$ kpc). We therefore restrict ourselves to values of μ_{cl} less than the critical value. On the other hand, if we adopt too low a value of μ_{cl}, the single galaxy image separations are only nominally increased. We present in Table 5 two typical solutions. The first solution is for a moderate value of μ_{cl}, whereas in the second solution we have adopted a value of μ_{cl} which is quite close to (but of course less than) the critical value. The masses and velocity dispersions for other values of Z can be obtained from the

© American Astronomical Society • Provided by the NASA Astrophysics Data System

1984ApJ...276..440S

TABLE 5

TWO TYPICAL SOLUTIONS FOR A GALAXY + CLUSTER LENS MODEL

Parameter	I(Galaxy + Cluster)	II(Galaxy + Cluster)
Z	0.1	0.5
μ_g	50	100
μ_{cl}	250	850
n_g	20	20
n_{cl}	10	10
R	200	250
u	(50.0, 50.0)	(60.0, 60.0)
Source	(18.0, 18.0)	(51.4, 42.8)
Images:		
a	(8.246, 8.246)	(27.578, −29.691)
c	(−0.497, −0.497)	(−0.203, −0.298)
b	(−2.171, −2.171)	(−5.547, 8.475)
Amplification:		
a	2.809	15.003
c	0.035	0.004
b	−0.490	−2.638
I_a/I_b	5.739	5.688
I_c/I_b	0.0714	0.0015
$M_g\ (M_\odot)$	7.4×10^{11}	6.2×10^{11}
$M_c\ (M_\odot)$	7.4×10^{14}	1.3×10^{15}
σ_g (km s^{-1})	354	336
σ_c (km s^{-1})	918	1138
r_c (kpc)	1.042	0.973
R_c (kpc)	208.4	243.25
$t_b - t_a$ (yr)	0.687	1.666

same solutions by suitable scaling (since μ_g, μ_{cl}, and R fix the solution). For example, for $Z = 0.18$, solution II in Table 5 gives $M_g = 2.2 \times 10^{11}\ M_\odot$, $\sigma_g = 283$ km s^{-1}, $M_c = 4.7 \times 10^{14}\ M_\odot$, $\sigma_c = 958$ km s^{-1}, $r_c = 0.493$ kpc, $R_c = 123$ kpc, and $t_b - t_a = 0.48$ years. This solution, however, has too low a value for the core radius of the cluster to be acceptable. Further, our computations show that the cluster enhances the intensity of the images produced by the galaxy, the degree of enhancement being higher for values of μ_{cl} closer to $\mu_{critical}$. The cluster does not, however, affect all the images to the same extent, and we were forced to consider more complicated image configurations in solution II than for the solutions presented in the previous sections, in order to explain the observed intensity ratios. Finally we note from Table 5 that even though the presence of a cluster eases somewhat the constraints on the parameters of the lenses, values of μ_{cl} close to the critical value are required for the effect to be decisive.

V. DISCUSSION AND CONCLUSIONS

It is evident that the observed image separation in the newly reported lensed quasar Q2345+007A,B sets stringent constraints on possible theoretical lens models. Among the gravitational lens models that we considered, the one involving two intervening galaxies (the double lens) seems to require the most reasonable values of the redshifts, masses, and velocity dispersions for the lens galaxies. Although the single lens models with the deflector situated at a redshift of $Z_d = 0.1$ cannot be ruled out, the parameters required to produce the observed features of Q2345+007A,B do seem to be rather extreme. The presence of a cluster at the same redshift as the single galaxy leads to an increase in the image separation to a moderate extent as well as to a magnification of image intensities. But the effect of the cluster turns out to be decisive only if the cluster constant μ_{cl} is close to the critical value. In this case the lens can be pushed out to redshifts of ~ 0.5 and still retain acceptable values for the parameters of the galaxy and the cluster.

Apart from the question of whether reasonable values for the parameters of the lens components obtain in a particular lens model, one must also consider the relative probability of each scenario. At first sight the double lens scenario appears less favourable compared to the one involving a single lens. However, there is another effect that comes into play in the case of the double lens. This is due to the fact that when two galaxies act as deflectors, the source may be much more misaligned from the projected lens center, compared to the case when there is only a single deflector, and still produce multiple images. The cross section for the double lens is thus larger than for the single lens. This is illustrated by the type II solutions of the double lens, for which, as was pointed out earlier, the projected source position can be as much as ~ 10 kpc from the centers of the lens galaxies. In this case the number of galaxies (within a cylinder of radius $R_g \sim 10$ kpc) between the QSO at a redshift Z_s and the observer is (Bahcall and Spitzer 1969; Bahcall and Peebles 1969 is

$$N = 0.08(R_g/10\ \text{kpc})^2(N_g/0.1\ \text{galaxy Mpc}^{-3})[(1 + Z_s)^2 - 1]\ .$$

Here N_g is the average number density of all galaxies, and we have assumed a cosmological model with $q_0 = 0$ and $H_0 = 60$ km s^{-1} Mpc^{-1}. For a redshift $Z_s = 2.15$ and a choice of $N_g = 0.01$ galaxy Mpc^{-3}, which might be more appropriate for the massive galaxies that we need for modeling, N comes out to be ~ 0.07. A rough estimate of the probability for the double lens is then given by $N^2F \approx 0.12\%$. Here $F \approx r^2/R_g{}^2$ takes into account the fact that for the double lens to be effective, (*a*) the amount of misalignment $|u|r_c$ cannot exceed $r(\sim 5$ kpc), and (*b*) one of the two deflectors should be within a certain angular distance of the line joining the source and the other deflector. In the case of type I solutions for the double lens, the probabilities are lowered. However, the net amplification of the source intensity by a factor of ~ 40 favors the detection of such events in flux-limited samples.

Future observational tests can provide ways of deciding the nature of the lens. One such test is the detection of a lens galaxy with a redshift greater than ~ 0.14. This would virtually rule out the single lens model, and if a cluster or at least some more galaxies are not observed in the neighborhood, this would favor the double lens model. On the other hand, if no intervening lens galaxy is detected, it would not auger well for the lens scenario, especially those involving galaxies as lenses, unless a large value of M/L for the galaxy is invoked.

The time delay between the images also proves to be important in distinguishing between various lens models. It is interesting to note that while the time delay $t_b - t_a$ is negative for the single lens model, it is positive for all the solutions that we computed with the double lens and with the cluster. Here *a* refers to the bright image and *b* to the fainter one, and the positive value of $t_b - t_a$ implies that the intensity variations of image *b* follow those in image *a*. The difference in sign of the time delay is essentially related to the fact that the observed intensity ratio of 4–6 could be achieved in the single lens model

© American Astronomical Society • Provided by the NASA Astrophysics Data System

1984ApJ...276..440S

only by making the two "internal images" close together representing the bright image *a*. With the introduction of a cluster, however, this situation gets reversed, and the external image, which is farther out from the center of the galaxy, can be the brightest of the images, thus switching the sign of the time delay.

It should be pointed out at this stage that even with the double lens model or with a model involving a cluster component one can still find image configurations where the bright image consists of two images very close together. In such a situation, the time delay $t_b - t_a$ will again be negative. A positive time delay for $t_b - t_a$ can thus rule out the single lens model, although the observation of a negative $t_b - t_a$ does not rule out the double lens models. Moreover, if future interferometric observations are unable to resolve the bright image into individual components separated by $\sim 0''.1$, then our models predict that the time delay $t_b - t_a$ must necessarily be positive.

Finally, the magnitude of the time delay can also further distinguish between various lens models. Thus, type I double lens models predict a time delay $t_b - t_a$ of a few months, while for type II the time delay is of the order of 3–4 years. The models involving a cluster component predict time delays between these two values, of the order of 1 year. Until the deflectors are found en route to the quasar, effectively bending the light rays reaching the observer, and until the time delay measurements show the expected effects of the intervening deflectors, the gravitational lenses will continue to remain in the realm of hypothesis.

We are grateful to D. Narasimha, J. V. Narlikar, J. P. Ostriker, and M. J. Rees for valuable discussions and helpful comments.

REFERENCES

Bahcall, J. N., and Peebles, P. J. E. 1969, *Ap. J. (Letters)*, **156**, L7.
Bahcall, J. N., and Spitzer, L. 1969, *Ap. J. (Letters)*, **156**, L63.
Bourassa, R. R., and Kantowski, R. 1975, *Ap. J.*, **195**, 13.
Bourassa, R. R., Kantowski, R., and Norton, T. D. 1973, *Ap. J.*, **185**, 747.
Cooke, J. H., and Kantowski, R. 1975, *Ap. J. (Letters)*, **195**, L11.
Gott, J. R., and Gunn, J. E. 1974, *Ap. J. (Letters)*, **190**, L105.
King, I. R. 1972, *Ap. J. (Letters)*, **174**, L123.
Narasimha, D., Subramanian, K., and Chitre, S. M. 1982, *M.N.R.A.S.*, **200**, 941 (Paper I).
Refsdal, S. 1964, *M.N.R.A.S.*, **128**, 295.
Walsh, D., Carswell, R. F., and Weymann, R. J. 1979, *Nature*, **279**, 381.
Weedman, D. W., Weymann, R. J., Green, R. F., and Heckman, T. M. 1982, *Ap. J. (Letters)*, **255**, L5.
Weymann, R. J., Latham, D., Angel, J. R. P., Green, R. F., Liebert, J. W., Turnshek, D. A., Turnshek, D. E., and Tyson, J. A. 1980, *Nature*, **285**, 641.
Wilkinson, J. H. 1965, *The Algebraic Eigenvalue Problem* (Oxford: Clarendon Press).
Young, P., Gunn, J. E., Kristian, J., Oke, J. B., and Westphal, J. A. 1981, *Ap. J.*, **244**, 736.

Note added in proof.—Some recent searches for a lens in the direction of Q2345+007 by Sol *et al.* and Keel (Liège Symposium on Quasars and Gravitational Lenses, 1983) do not reveal any lens object to a limiting R magnitude of 21.5 (Sol *et al.*) and 23 (Keel). Assuming the lens to be a cluster containing a first-rank elliptical or cD galaxy, Keel places the lens at a redshift $Z > 1.0$ (with $H_0 = 50$ km s^{-1} Mpc^{-1} and $q_0 = \frac{1}{2}$). The corresponding limit given by Sol *et al.* is $Z > 0.5$, if the lens galaxy is a member of a group.

With a view to accommodate these constraints we have done further modeling to find that the single lens model is certainly ruled out. The double lens model involving two galaxies at different redshifts can explain the observations only if the galaxy mass is pushed to $\gtrsim 25 \times 10^{11}\ M_\odot$ and the velocity dispersion $\sigma_g \sim 390$ km s^{-1}. The lens can then be placed at a redshift $Z \sim 0.7$.

The model which seems to account for the observations best is the one involving a galaxy at the center of a rich cluster, in which case the lens can be placed at a redshift $Z \gtrsim 1.0$. In particular, a solution with the following set of parameters for the lens at $Z = 1$: $\sigma_g = 336$ km s^{-1}, $\sigma_c = 1150$ km s^{-1}, $M_g = 18 \times 10^{11}\ M_\odot$, $M_c = 1.1 \times 10^{15}\ M_\odot$:

$$r_c = 3 \text{ kpc}, \qquad R_c = 200 \text{ kpc},$$

gives a separation of images $\sim 7''.27$, $I_a/I_b = 4.24$, and $I_c/I_b = 0.013$. The total amplification ($|I_a| + |I_b| + |I_c|$) is 32.564, and the time-delay ($t_b - t_a$) comes out to be 3.995 years. Clearly this model accounts for the observed constraints in a satisfactory manner. Further, the total intensity amplification of ~ 33 will selectively favor such a lensed quasar in flux-limited samples.

S. M. Chitre and K. Subramanian: Theoretical Astrophysics Group, Tata Institute of Fundamental Research, Homi Bhabha Road, Bombay 400005, India

© American Astronomical Society • Provided by the NASA Astrophysics Data System